Influence of sulfide nanoparticles on dissolved mercury and zinc quantification by diffusive gradient in thin-films (DGT) passive samplers

Anh Le-Tuan Pham [1, £,] *, Carol Johnson [1], Devon Manley [1], and Heileen Hsu-Kim [1,]*

[1] Department of Civil and Environmental Engineering, Duke University, Durham, NC 27503, USA

[£] Current address: Department of Civil and Environmental Engineering, Carleton University, Ottawa, ON K1S 5B6, Canada

Supporting Information

(Manuscript prepared for submission to Environmental Science and Technology)

13 pages, Tables S1 & S2, and Figures S1 – S6.

*Corresponding authors: Anh Le-Tuan Pham (email: a.pham@carleton.ca; phone: +1-613-520-2600 (ext. 2984); Heileen Hsu-Kim (email: hsukim@duke.edu; phone +1-919-660-5109).

17 **A. Speciation of dissolved Hg(II) and Zn(II) in the DGT uptake experiments.** The speciation

18 of dissolved Hg(II) and Zn(II) were calculated employing equilibrium constants shown in Table

19 S1 and S2, respectively, and were performed with MINEQL+ (v. 4.6) [1].

20

21 **Table S1.** Stability constants employed to calculate the speciation of dissolved Hg(II) in the
22 DGT uptake experiments. The concentrations of Hg(II) and ligands in the calculation were as
23 follow: [total dissolved Hg(II)] = 5 nM; $[NO_3^-]$ = 10 mM; [SRHA] = 1 mgC/L = 1.34 μM
24 (assuming that the C content of SRHA is 53 wt.%, and the molecular weight of SRHA is 1399
25 Da) [2]; pH = 7.6.
26
27 *MINEQL+ predicted that 100% of Hg in the solution is associated with SRHA*.
28

Reaction	Log K	Reference
$Hg^{2+} + H_2O \Leftrightarrow HgOH^+ + H^+$	-3.40	1
$Hg^{2+} + 2\ H_2O \Leftrightarrow Hg(OH)_2^0 + 2H^+$	-6.2	1
$Hg^{2+} + 3H_2O \Leftrightarrow Hg(OH)_3^- + 3H^+$	-21.1	1
$Hg^{2+} + NO_3^- \Leftrightarrow HgNO_3^+$	-0.434	1
$Hg^{2+} + 2NO_3^- \Leftrightarrow Hg(NO_3)_2^0$	-0.814	1
$Hg^{2+} + SRHA \Leftrightarrow HgSRHA$	22.5	2

29

30 **Table S2.** Stability constants employed to calculate the speciation of dissolved Zn(II) in the
31 DGT uptake experiments. The concentrations of Zn(II) and ligands in the calculation were as
32 follow: [total dissolved Zn(II)] = 1 µM; [NO_3^-] = 10 mM; [SRHA] = 1 mgC/L = 1.34 µM
33 (assuming that the C content of SRHA is 53 wt.%, and the molecular weight of SRHA is 1399
34 Da) [2]; pH = 7.6.

35 *MINEQL+ predicted that ca. 31% of Zn in the solution is associated with SRHA, while 65%,*
36 *2.5%, and 1.5% of Zn exists as Zn^{2+}, $ZnOH^+$, and $ZnNO_3^+$, respectively.*

37

Reaction	Log K	Reference
$Zn^{2+} + H_2O \Leftrightarrow ZnOH^+ + H^+$	-9.0	1
$Zn^{2+} + 2 H_2O \Leftrightarrow Zn(OH)_2^0 + 2H^+$	-17.8	1
$Zn^{2+} + 3H_2O \Leftrightarrow Zn(OH)_3^- + 3H^+$	-28.1	1
$Zn^{2+} + 4H_2O \Leftrightarrow Zn(OH)_4^- + 4H^+$	-40.5	1
$Zn^{2+} + NO_3^- \Leftrightarrow ZnNO_3^+$	0.3	1
$Zn^{2+} + 2NO_3^- \Leftrightarrow Zn(NO_3)_2^0$	-0.4	1
$Zn^{2+} + (SRHA_1) \Leftrightarrow Zn(SRHA_1)$	5.25*	3
$Zn^{2+} + (SRHA_2) \Leftrightarrow Zn(SRHA_2)$	6.86*	3

38

39 *We performed a thorough literature search for the stability constants of Zn-SRHA complexes
40 but were not able to find one. Therefore, the stability constant values reported by Cheng and
41 Allen (2006) [3], who studied zinc complexation by dissolved organic matter from different
42 surface waters, were employed in our calculation. In the study by Cheng and Allen, the Zn-NOM
43 titration data was best fitted by a 2-site model in which NOM is consisted of two types of
44 binding site (denoted as $SRHA_1$ and $SRHA_2$ in Table S2). The average site concentrations and
45 the respective stability constant values reported by Cheng and Allen (Table 2 in that study) [3]
46 were utilized for Zn(II) speciation calculation. They are: [$SRHA_1$] = 2.06 mmol/g C = 2.06 µM;
47 [$SRHA_2$] = 0.12 mmol/g C = 0.12 µM; $logK_{Zn(SRHA1)}$ = 5.25; $logK_{Zn(SRHA2)}$ = 6.86.

B. Characterization of HgS and ZnS nanoparticles. Transmission electron microscopy (TEM) was used to image and analyze the nanoparticles for size, composition (via energy dispersive spectroscopy, EDS), and structure (via selected area electron diffraction, SAED, and fast Fourier transform of high resolution images, FFT). TEM grids (ultrathin carbon film, ~3-5 nm thick, on copper mesh) held by reverse-action tweezers were dipped into the nanoparticle suspensions, swirled for a few seconds, removed, wicked gently with a lint-free wipe, and rinsed two times with ultrapure water to remove salts. The wicking process helps prevent aggregation via the "coffee ring" drying effect. Grids were analyzed on a JEOL 2100 operated at 200kV. HgS nanoparticles are shown in Figure S1. The average particle size is 6.3(±2.3) nm as measured from 29 particles in 5 images, and particles are generally dispersed though sometimes appear in loose aggregates (possible drying artifact). Both SAED and FFT patterns are insufficient to identify whether the HgS particles are cinnabar or metacinnabar, which agrees with previous work using EXAFS showing that the Hg-S bond distance is in-between that of cinnabar and metacinnabar.[4]
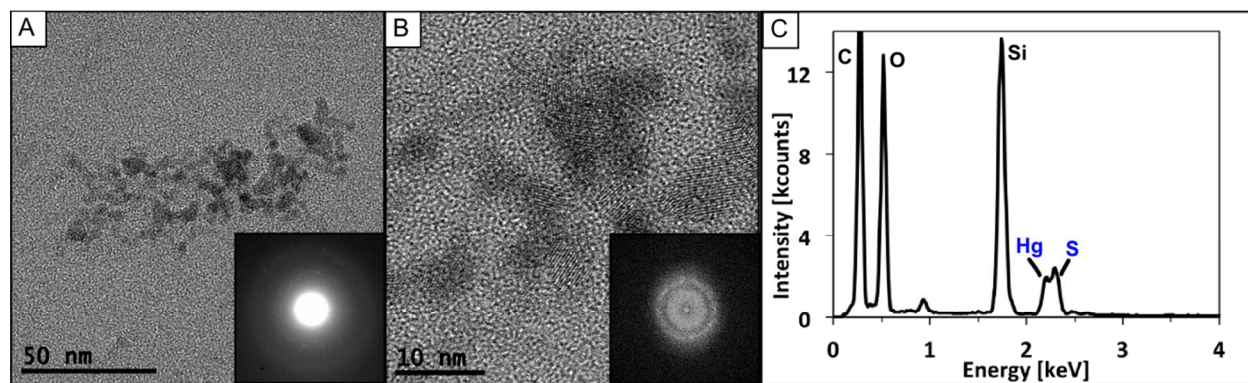

Figure S1. TEM of HgS nanoparticles, 3 days aged. (A) TEM image of an aggregate of ~ 5 nm HgS, with an inset of the SAED pattern showing a few crystalline spots; (B) high resolution (HR-TEM) image of the same particles with lattice fringes visible indicating crystallinity, with an inset of the FFT of that image showing crystalline spots as well. (C) EDS spectrum verifying that the particles are composed of Hg and S. The source of the Si peak is unknown but could be contamination from water or glassware.

69 ZnS nanoparticles are shown in Figure S2. The average size is 3.7(±1.5) nm as measured from

70 43 particles in 3 images, and particles are very dispersed throughout the grid. Their dispersity

71 and extremely small size made it extremely difficult to get enough signal for EDS and SAED,

72 and only the rare large aggregate allowed for these analyses (Figure S2B and C). The crystalline

73 phase could not be conclusively identified as wurtzite or sphalerite by SAED. High resolution

74 TEM was also difficult and did not reveal any lattice fringes, but particles of that size can be

75 quite unstable under the electron beam. These results match with previous studies on HgS and

76 ZnS nanoparticles.[4,5]
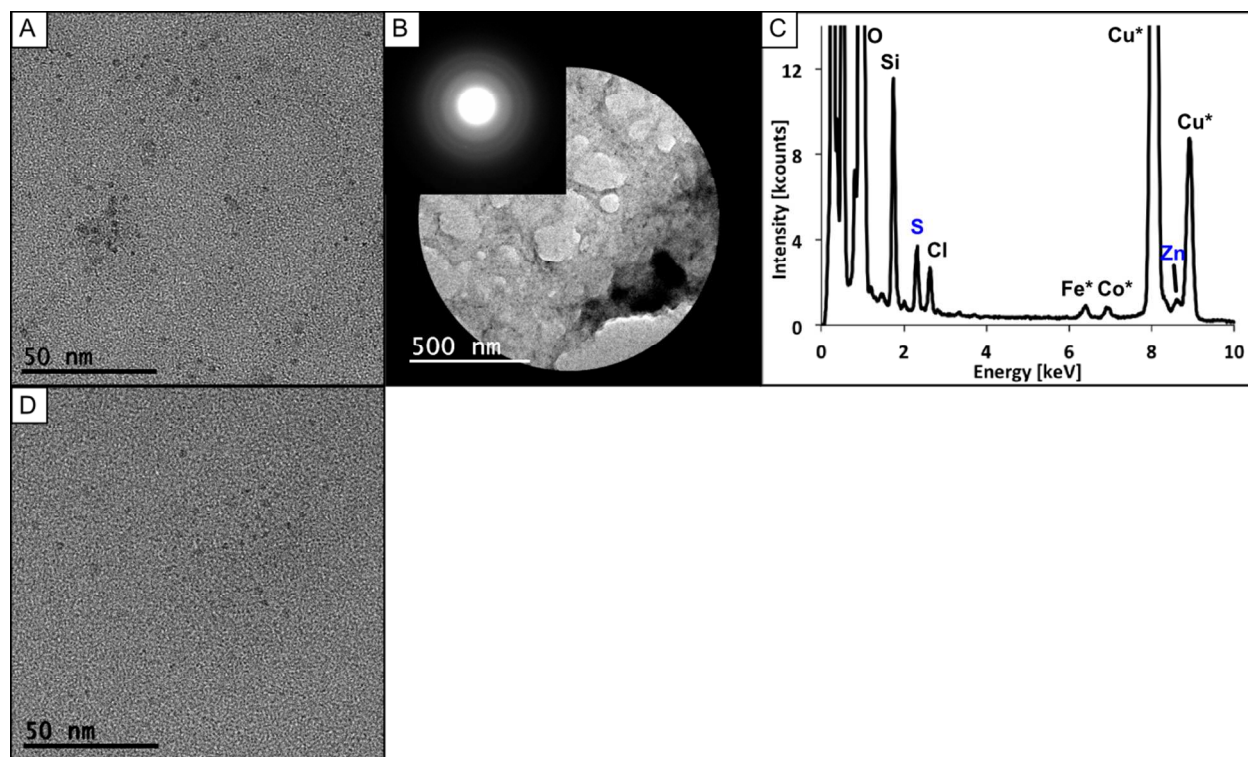
77

78

79 **Figure S2.** TEM of ZnS nanoparticles, fresh (A-C) & 4 days aged (D). (A, D) TEM images
80 showing monodispersed nanoparticles smaller than 5 nm; (B) image of a thick aggregate of
81 Suwanee River Humic Acid (SRHA) and ZnS nanoparticles (selected area aperture visible) with
82 an inset of the SAED pattern; (C) EDS spectrum showing the presence of Zn and S (Fe and Co in
83 equal heights are from the instrument, Cu is from the TEM grid).
84

85 **C. Synthesis of 3-mercaptopropyl functionalized silica gel (Si-SH)**. Si-SH beads were

86 synthesized in our laboratory according to the procedure reported in Quang *et al.*[6] Briefly, 5

87 grams of silica gel (200 – 400 mesh, Sigma Aldrich Inc.) was added to a mixture of 2 g H_2O, 5 g

88 ethanol, and 3 g 3-mercaptopropyltrimethoxysilane (Aldrich). The resulted suspension was aged

89 at 50 ºC for 40 h, and the supernatant was decanted to retrieve the Si-SH beads. In the final step,

90 the Si-SH beads were washed 3 times with ethanol and freeze-dried.

91 **D. Preparation of the DGT sampler.** The samplers consisted of a 0.45 µm nitrocellulose

92 membrane filter (Fisher Scientific), an agarose diffusion layer, and a metal binding layer

93 enclosed in a plastic casing that was purchased from DGT Research Ltd. (Lancaster, UK) The

94 agarose diffusion layer was prepared by dissolving 0.15 g of agarose in 10 g of water, and the

95 solution was cast between two glass plates that were separated from each other by 0.75 mm-thick

96 spacers. After 1 h, the agarose gel was retrieved and cut into small disks ready for DGT sampler

97 assembly. The obtained agarose gel was 0.75 mm thick, which is a typical thickness of diffusion

98 layer used in DGT sampler.

99   The binding layer was prepared by mixing 2 g of the Si-SH beads with 10 g of solution of

100 15% acrylamide/bis acrylamide. Polymerization was initiated by adding 70 µL of an aqueous

101 solution of 1% ammonium persulfate $(NH_4)_2S_2O_8$ and 40 µL of tetramethylethylenediamine,

102 and the suspension was cast between two glass plates that were separated from each other by

103 0.75 mm-thick spacers. After approximately 1.5 h, the obtained Si-SH-containing

104 polyacrylamide gel (*i.e.*, the binding layer) was retrieved and cut into small disks. The disks were

105 hydrated in 10 mM $NaNO_3$ for 24 h and subsequently used for DGT sampler assembly.

106 **E. Metal uptake tests to examine the performance of the binding layer.** The ability of the

107 binding layer disks in binding Zn and Hg was examined by submerging them into solutions of

108   different concentrations of dissolved Zn(II) and Hg(II), and measuring for mass of metals

109   accumulated on each disk. In the Zn uptake study, experiments were conducted in 15 mL plastic

110   centrifuge tubes containing 10 mL of solution of 10 mM $NaNO_3$ (background electrolyte), 2 mM

111   HEPES (buffer, pH = 7.6 – 7.7), and 5 – 40 μM $Zn(NO_3)_2$. A binding layer disk was added to

112   each test tube, and the tube was tumbled end-over-end for 3 days. Subsequently, the binding

113   layer was retrieved and digested with a mixture of 1:1 (v/v) of 37 wt.% HCl and 70 wt.% HNO_3

114   stock solutions, and the amount of Zn in the digestate was quantified using inductively coupled

115   plasma mass spectrometry (ICP-MS). The amount of Zn remaining in the test solution was also

116   quantified in order to complete mass balance and predict the amount of Zn that should have

117   accumulated on the binding layers.

118   The Hg uptake study was carried similarly to the Zn uptake study, with the following

119   modifications: 1) experiments were conducted in 44 mL certified Hg-free glass vials (Merx-T,

120   brand) containing 40 mL of solution of 10 mM $NaNO_3$ (background electrolyte), 0.5 mM

121     $NaHCO_3$ (buffer, pH = 7.6 – 7.7), and 1 – 10 nM $Hg(NO_3)_2$; 2) the test tubes were tumbled end-

122   over-end for 5 days; 3) Hg was measured using cold vapor atomic fluorescence spectrometry

123   following method 1631 (Environmental Protection Agency)[7]; and 4) both the amounts of Hg

124   remained in the test solution and Hg sorbed to the test tube walls were quantified to complete

125   mass balance and predict for the amount of Hg that should have accumulated on the binding

126   layers.

127   The results of these experiments, presented in Figure S2 and S3, indicated that the binding

128   layers were effective in taking up Zn and Hg, and that digestion by aqua regia was effective in

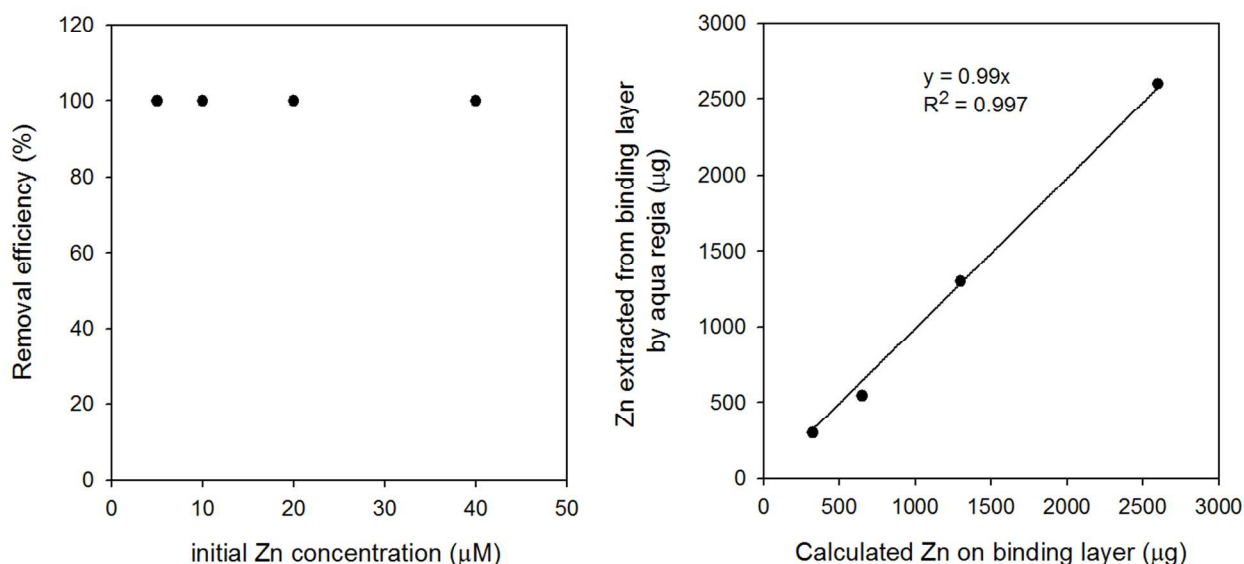129   eluting the bound metals from the binding layers.

130

Figure S3. Removal efficiency of dissolved Zn(II) by binding layer disks from solutions containing $[Zn(II)]_0 = 5 - 40$ μM (left), and elution efficiency by aqua regia (right). An elution efficiency of 99% was obtained. The amounts of Zn accumulated on the binding layers (the x-axis of the figure on the right) were calculated by subtracting the mass of Zn(II) left from the amount initially present in the solution.
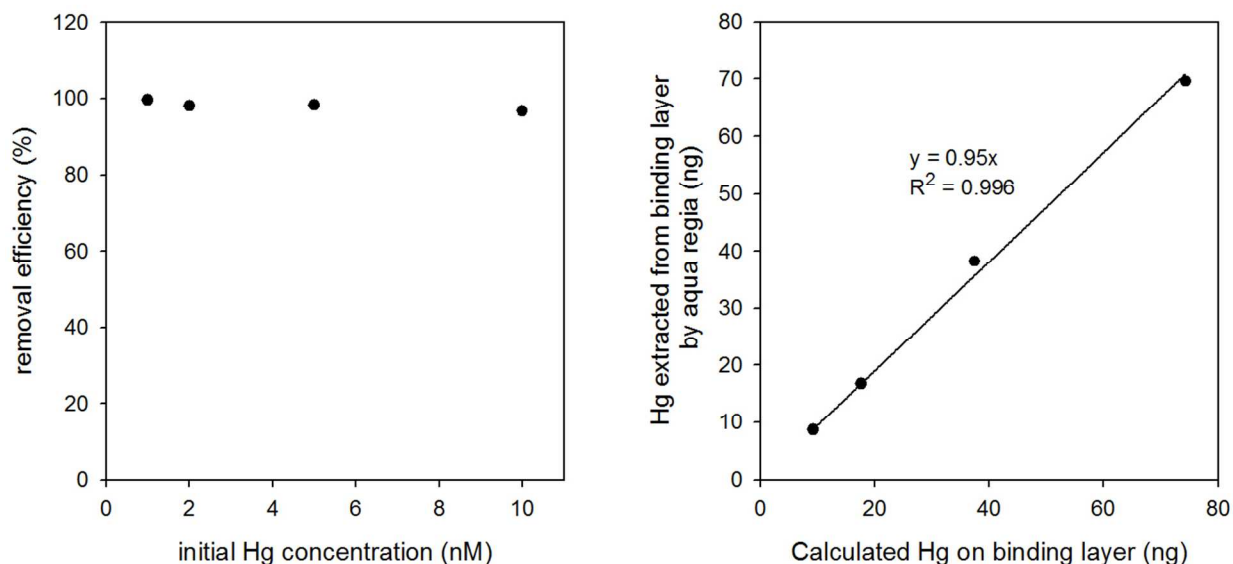

136

Figure S4. Removal efficiency of dissolved Hg(II) by binding layer disks from solutions containing $[Hg(II)]_0 = 1 - 10$ nM (left), and elution efficiency by aqua regia (right). An elution efficiency of 95% was obtained. The amounts of Hg accumulated on the binding layers (x-axis of the figure on the right) were calculated by subtracting the massed of Hg(II) left in the solution and adsorbed on the test tube walls from the amount initially present in the solution.

142 **F. Elution of metals from the filter and agarose layers.** In the DGT uptake experiments, Zn

143 and Hg accumulated on the filter and agarose layers were eluted by acid solutions of 0.19 wt.%

144 HCl and 1.4 wt.% HNO_3 (for elution of metals on the filters), or 37 wt.% HCl (for metal release

145 following complete dissolution of agarose).

146 **G. Calculation of diffusion coefficient *D*.** The diffusion coefficients were calculated employing

147 the rearranged form of equation (1) in the main text:

$$\frac{m}{C_b} = \frac{D \times A}{\Delta g} \times t \qquad (2)$$

148 where *m* is mass of metal accumulated on the binding layer, C_b is the concentration of dissolved

149 metal in the bulk solution (measured by filtration or anodic stripping voltammetry), D is the

150 diffusion coefficient, A is the sampling area (A = 3.14 cm^2), t is the deployment time, and Δg is

151 the thickness of the diffusion layer (*i.e.*, Δg = the thickness of agarose diffusion layer +

152 membrane filter + stagnant liquid layer on the surface of the DGT sampler = 0.75 + 0.15 + 0.53[*]

153 = 1.43 mm).

154 Based on equation (2), the slopes of the regression lines in Figure 1C and 2C are equaled to $\frac{D \times A}{\Delta g}$.

155 Thus, the diffusion coefficients *D* can be readily calculated.

156

157 [*] The thickness δ of the stagnant liquid layer was determined according to the procedure

158 described by Zhang and Davison.[8] Briefly, δ can be determined by conducting DGT uptake

159 experiments using samplers constructed from agarose diffusion layers that have different

160 thickness, and employing the rearranged form of equation (1):

$$\frac{1}{m} = \frac{\Delta \alpha}{D \times C_b \times t \times A} + \frac{\delta}{D \times C_b \times t \times A} \qquad (2)$$

161   where $\Delta\alpha$ = the thickness of agarose layer + membrane filter. $\Delta\alpha$ can be varied by using agarose

162   layers of different thicknesses. Thus, δ can be determined by plotting $1/m$ vs. $\Delta\alpha$. From a Zn

163   uptake test, δ was found to be 0.53 mm under experimental conditions employed in this study

164   (Figure S5).

The plot shows:

$$y = 1.31x + 0.70$$
$$R^2 = 0.89$$

y-axis: $1/m$ (μg^{-1})

x-axis: $\Delta\alpha$ (total thickness of agarose and filter) (mm)
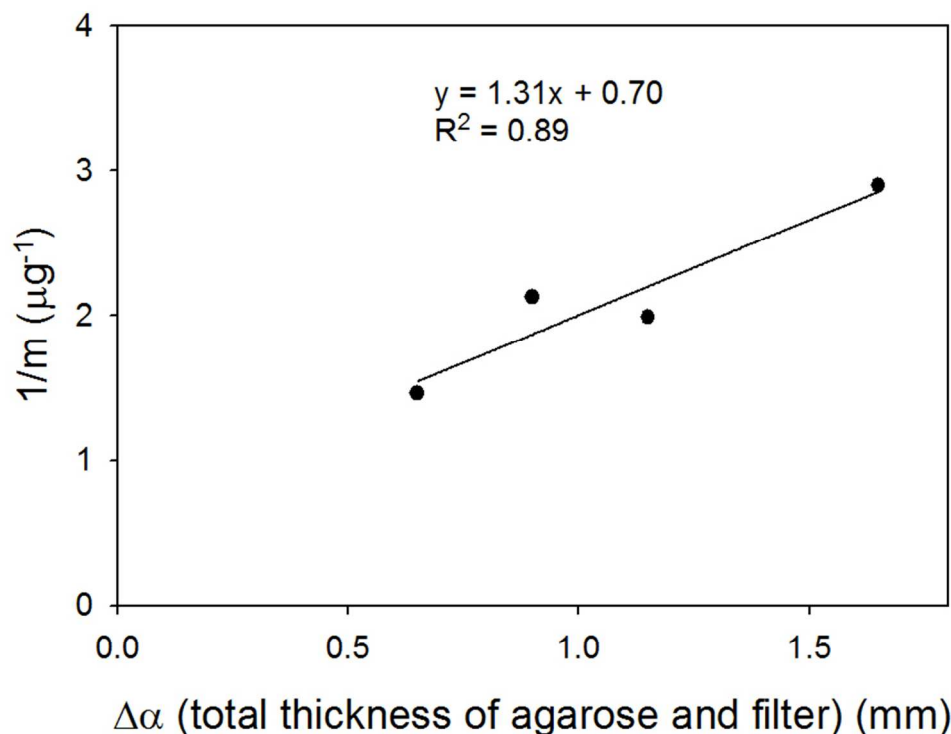
165

166   **Figure S5.** Uptake of dissolved Zn(II) by DGT samplers constructed with agarose layers of
167   different thicknesses (i.e., 0.5, 0.75, 1, and 1.5 mm). All solutions contained 10 mM NaNO$_3$, 2
168   mM HEPES (pH = 7.5 – 7.7), and 1 μM Zn(NO$_3$)$_2$. After 22 h, DGT samplers were retrieved to
169   determine the mass of Zn accumulated on the binding layer (m). Using the intersection and slope
170   of the regression line, the thickness δ of the stagnant liquid layer was found to be δ = 0.7/1.31 =
171   0.53 mm.

172

173

174
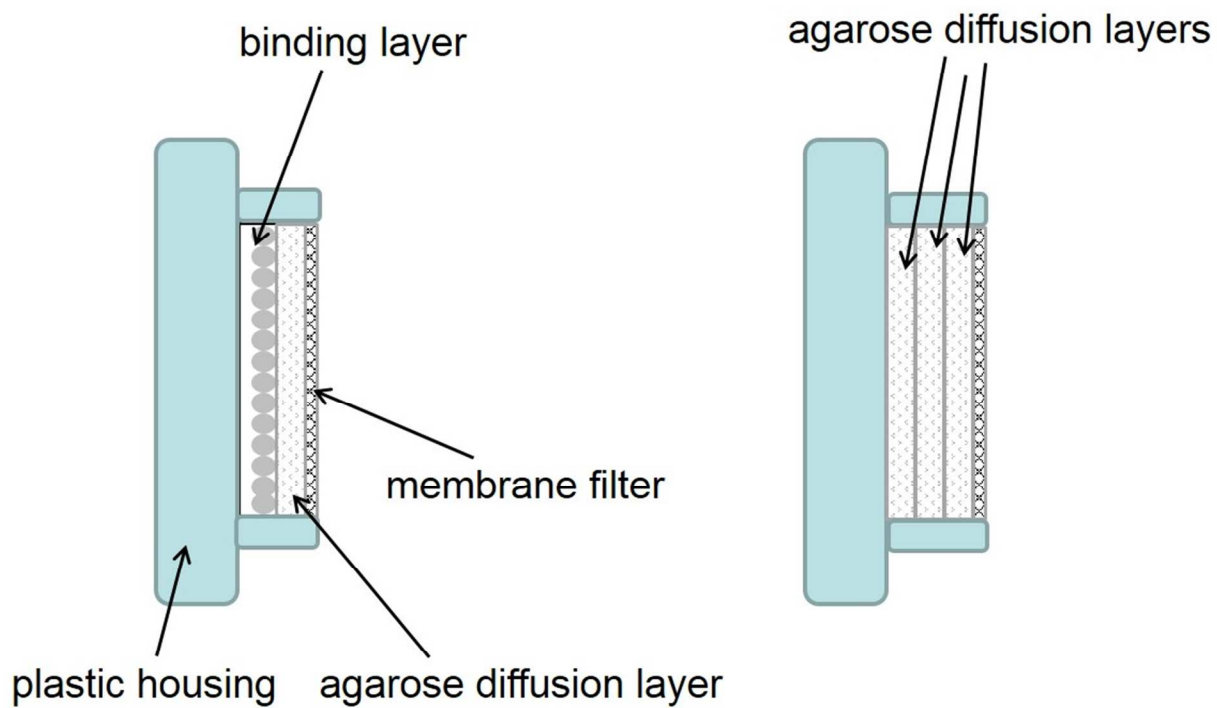
Figure S6. The structure of a normal DGT sampler (left) and a modified DGT sampler (right).
The modified sampler (m-DGT) has three agarose diffusion layers but no binding layer.

178 **References**

179 1. Schecher, W. D., MINEQL+: A chemical equilibrium program for personal computers;

180 Environmental Research Software, Hallowell, ME. 2001.

181 2. Haitzer, M.; Aiken, G. R.; Ryan, J. N.; Binding of Mercury(II) to Aquatic Humic Substances:

182 Influence of pH and Source of Humic Substances. *Environmental Science and Technology*. **2003,**

183 37, 2436-2441.

184 3. Cheng, T.; Allen, H. E.; Comparison of zinc complexation properties of dissolved natural

185 organic matter from different surface waters. *Journal of Environmental Management.* **2006**, 80,

186 222-229.

187 4. Pham, A. L.-T.; Morris, A.; Zhang, T.; Ticknor, J.; Levard, C.; Hsu-Kim, H. Precipitation of

188 nanoscale mercuric sulfides in the presence of natural organic matter: Structural properties,

189 aggregation, and biotransformation. *Geochimica et Cosmochimica Acta*. **2014**, 133, 204-215

190 5. Deonarine, A.; Lau B. L. T.; Aiken, G. R.; Ryan, J. N.; Hsu-Kim H. Effects of humic

191 substances on precipitation and aggregation of zinc sulfide nanoparticles. *Environmental Science*

192 *and Technology*. **2011**, 45 (8), 3196 – 3201.

193 6. Quang, D. V.; Lee, J. E.; Kim, J.; Kim, Y. N.; Shao, G. N.; Kim, H. T. A gentle method to

194 graft thiol-functional groups onto silica gel for adsorption of silver ions and immobilization of

195 silver nanoparticles. *Powder Technology*. **2013**, 235, 221-227.

196 7. *Method 1631, Revision D: Mercury in Water by Oxidation, Purge and Trap, and Cold Vapor*

197 *Atomic Fluorescence Spectroscopy*; U.S. Environmental Protection Agency: Washington, DC,

198 2001.

199   8. Zhang, H.; Davison, W. Performance characteristics of diffusion gradients in thin films for the

200   in situ measurement of trace metals in aqueous solution. *Analytical Chemistry*. **1995**, 67, 3391-

201   3400.